Electronic Supplementary Material (ESI) for Organic & Biomolecular Chemistry.

Supporting Information

Engineering a periplasmic binding protein for amino acid sensors with improved binding properties

Wooseok Ko, Sanggil Kim, Hyun Soo Lee*

Department of Chemistry, Sogang University, Seoul 121-742, Republic of Korea

Table S1. Measurement of the distances between the α-carbon of each residue (A142−E242) in the domain on the top in Figure 1 and the α-carbon of Asp1 in LBP and calculation of percent changes of the distances upon ligand binding. The distances between the two residues were measured using Pymol software, and the crystal structures of an *apo*-form (PDB ID: 1USG) and a ligand-bound form (PDB ID: 1USK) of LBP from the protein data bank (PDB) were used to measure the distances. The residues (A177, G178, and S232) showing distance change over 25% are shown in boldface.

Residue	Distance from Asp1 in the ligand-free form (Å)	Distance from Asp1 in the ligand-bound form (Å)	% change of the distance (%)
A142	58.95	55.59	5.70
I143	56.24	52.03	7.49
I144	57.05	50.20	12.01
H145	55.27	46.74	15.43
D146	56.32	44.80	20.45
K147	55.87	44.59	20.19
Q148	52.97	40.80	22.98
Q149	49.59	39.06	21.23
Y150	47.73	38.24	19.88
G151	50.29	41.64	17.20
E152	51.62	43.93	14.90
G153	48.15	42.34	12.07
L154	47.36	43.01	9.18
A155	50.85	46.49	8.57
R156	50.58	47.37	6.35
S157	47.31	46.13	2.49
V158	48.87	48.28	1.21
Q159	51.95	51.20	1.44
D160	49.97	51.03	−2.12
G161	48.13	50.95	−5.86
L162	51.28	53.85	−5.01
K163	53.35	55.83	−4.65
A164	50.72	55.47	−9.37
A165	51.09	57.47	−12.49
N166	54.89	59.73	−8.82
A167	55.55	59.08	−6.35
N168	58.80	60.65	−3.15
V169	58.27	58.03	0.41
V170	61.89	60.27	2.62
F171	61.41	57.76	5.94

F172	59.00	54.22	8.10
D173	60.24	52.91	12.17
G174	59.45	50.01	15.88
I175	61.00	49.39	19.03
T176	61.34	47.21	23.04
A177	**59.00**	**44.06**	**25.32**
G178	**61.11**	**44.71**	**26.84**
E179	63.41	48.41	23.66
K180	65.18	49.99	23.30
D181	67.61	53.49	20.88
F182	66.07	54.15	18.04
S183	69.42	57.91	16.58
A184	69.58	58.76	15.55
L185	66.05	56.77	14.05
I186	66.43	58.26	12.30
A187	69.85	61.73	11.62
R188	68.34	61.24	10.39
L189	65.62	60.11	8.40
K190	68.39	63.31	7.43
K191	70.65	65.68	7.03
E192	67.87	64.32	5.23
N193	66.81	64.28	3.79
I194	63.17	60.66	3.97
D195	61.06	59.77	2.11
F196	57.72	56.19	2.65
V197	56.80	53.28	6.20
V198	53.47	49.83	6.81
Y199	53.82	47.44	11.85
G200	51.40	44.32	13.77
G201	51.95	41.92	19.31
Y202	51.98	40.19	22.68
Y203	53.38	41.39	22.46
P204	56.81	42.69	24.85
E205	57.97	45.40	21.68
M206	56.49	46.32	18.00
G207	58.24	46.82	19.61
Q208	61.58	49.14	20.20
M209	61.29	51.09	16.64
L210	60.55	51.71	14.60
R211	63.44	52.97	16.50
Q212	65.86	55.34	15.97
A213	64.71	56.62	12.50
R214	65.28	57.72	11.58
S215	68.57	59.33	13.48
V216	69.94	61.98	11.38
G217	68.43	62.39	8.83
L218	65.83	60.65	7.87

K219	63.54	60.31	5.08
T220	60.94	57.88	5.02
Q221	57.28	55.16	3.70
F222	55.50	51.71	6.83
M223	51.85	48.60	6.27
G224	50.00	45.10	9.80
P225	46.60	41.66	10.60
E226	45.00	38.57	14.29
G227	47.44	37.87	20.17
V228	50.29	40.96	18.55
G229	48.53	40.17	17.23
N230	49.90	38.53	22.79
A231	51.42	39.45	23.28
S232	**54.58**	**40.62**	**25.58**
L233	54.98	43.29	21.26
S234	56.56	45.77	19.08
N235	58.54	45.42	22.41
I236	60.25	46.36	23.05
A237	60.40	48.98	18.91
G238	60.93	50.38	17.31
D239	61.02	52.99	13.16
A240	60.68	52.88	12.85
A241	56.91	49.64	12.77
E242	56.67	51.75	8.68

Fig. S1. The spectral overlaps of CouA and FPs. (A) Normalized absorption and emission spectra of CouA and EGFP. (B) Normalized absorption and emission spectra of CouA and YFP.

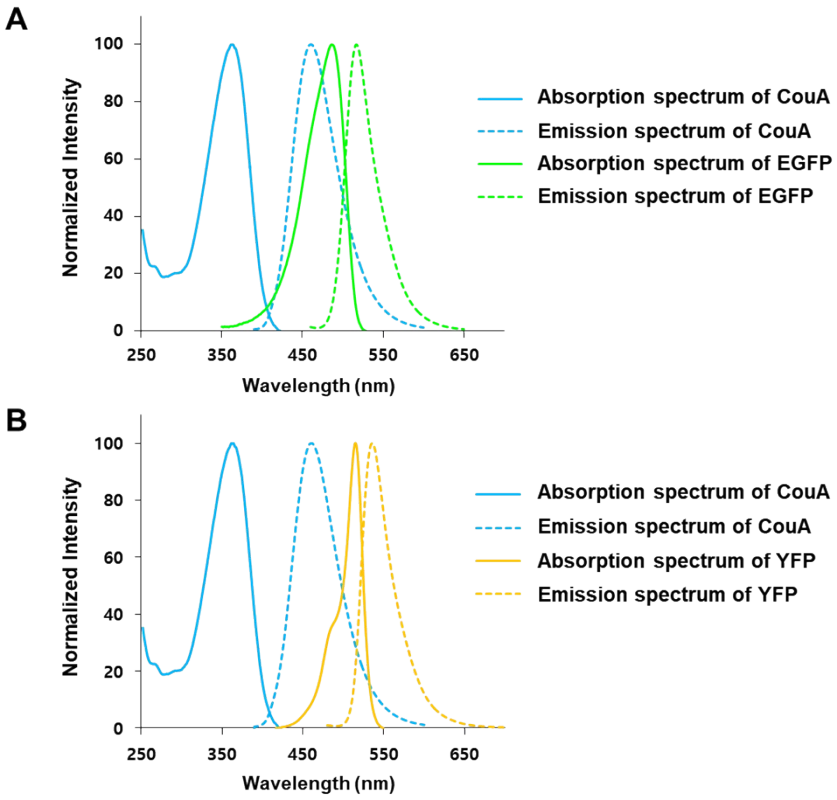

Fig. S2. SDS-PAGE analyses of purified sensor proteins. (A) EGFP-LBP and (B) YFP-LBP mutants containing CouA at A177 or G178 were expressed in presence of the corresponding tRNA/CouRS pair and CouA (1 mM), and purified by Ni-NTA affinity chromatography. The purified sensor proteins were analyzed by SDS-PAGE, and visualized by Coomassie-staining and fluorescence.

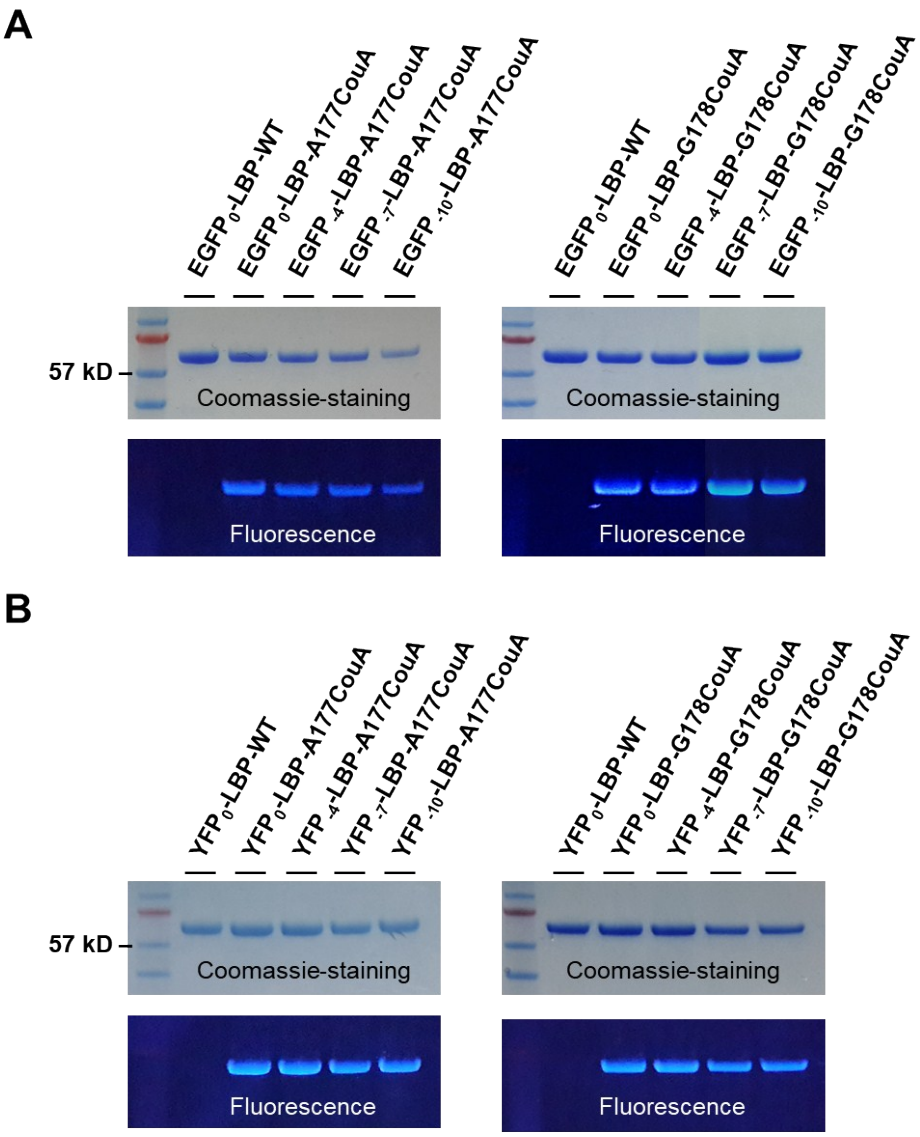

Fig. S3. (a) MALDI-TOF MS analyses of EGFP$_{-4}$-LBP-WT (Left) and EGFP$_{-4}$-LBP-G178CouA (Right): expected mass difference between EGFP$_{-4}$-LBP-WT and EGFP$_{-4}$-LBP-G178CouA is 188 Da and observed mass difference is 188 Da. (b) MALDI-TOF MS analyses of YFP$_{-10}$-LBP-WT (Left) and YFP$_{-10}$-LBP-G178CouA (Right): expected mass difference between YFP$_{-10}$-LBP-WT and YFP$_{-10}$-LBP-G178CouA is 188 Da and observed mass difference is 196 Da.

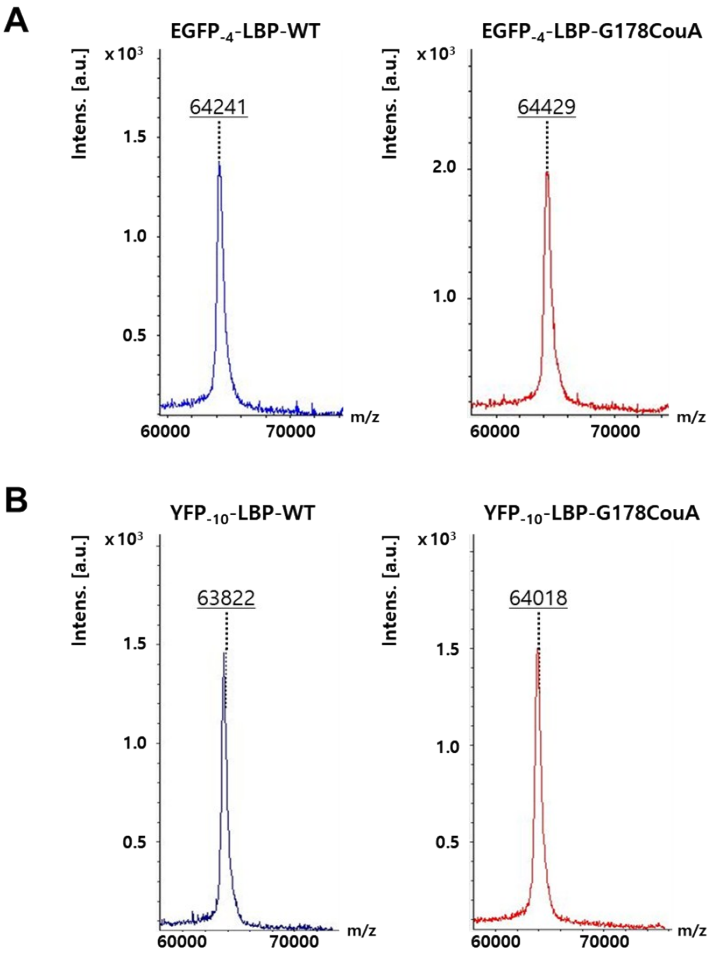

Fig. S4. Fluorescence spectra of the designed sensor proteins upon L-Leu binding. Fluorescence spectra for (A) EGFP-LBP sensor proteins and (B) YFP-LBP sensor proteins were measured at the indicated L-Leu concentrations with excitation at 360 nm. Assay conditions: 100 nM sensor protein, 50 mM phosphate buffer (pH 9.0), 50 mM NaCl, and L-Leu (indicated concentration).

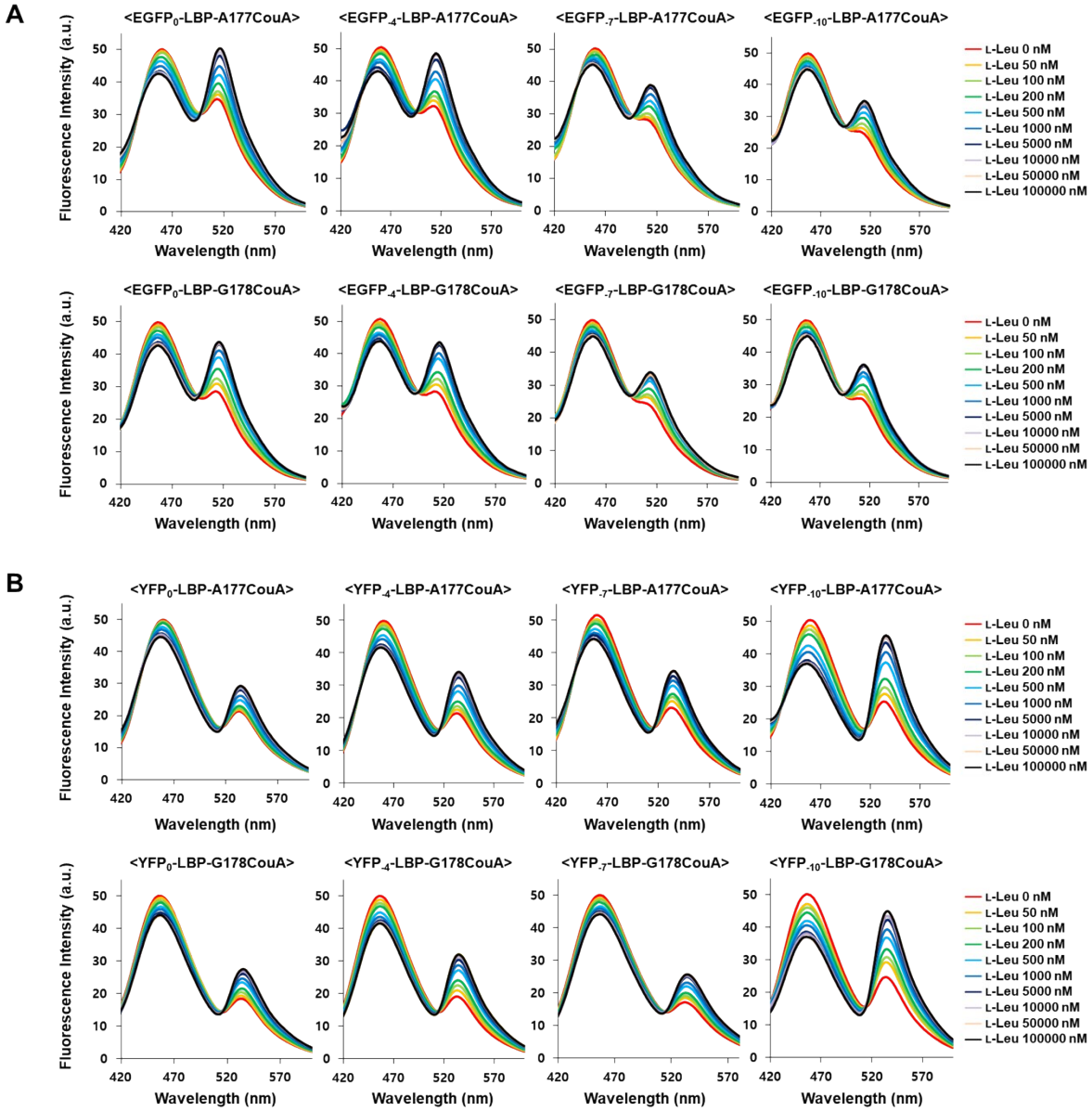

Table S2. The distances between CouA and the fluorophores of FPs calculated from FRET efficiency and Förster distance (r_0).

Sensor proteins	Distances between two fluorophores		Distance changes
	Apo-form	L-Leu bound form	
$EGFP_0$-LBP-G178CouA	65.13 nm	57.85 nm	7.28 nm
$EGFP_{-4}$-LBP-G178CouA	66.59 nm	58.75 nm	7.84 nm
$EGFP_{-7}$-LBP-G178CouA	65.22 nm	59.70 nm	5.52 nm
$EGFP_{-10}$-LBP-G178CouA	65.30 nm	59.65 nm	5.65 nm
YFP_0-LBP-G178CouA	64.20 nm	57.79 nm	6.41 nm
YFP_{-4}-LBP-G178CouA	64.25 nm	55.74 nm	8.51 nm
YFP_{-7}-LBP-G178CouA	64.47 nm	57.98 nm	6.49 nm
YFP_{-10}-LBP-G178CouA	64.48 nm	52.68 nm	11.8 nm

Fig. S5. (A) The ligand-binding site in the X-ray crystal structure of LBP complexed with L-Leu. W18 and the ligand, L-Leu, are shown. The figure was captured from PDB ID 1USK. (B) Evaluation of sensor proteins containing mutations in W18 for L-Leu binding. FRET ratio changes of each protein were calculated from $I_{\text{CouA, 468 nm}}$ and $I_{\text{YFP, 537 nm}}$ upon excitation at 360 nm in the presence (50 μM) and absence of L-Leu. Each data-point represents the average of three independent experiments. Assay conditions: 100 nM sensor protein, 50 mM phosphate buffer (pH 9.0), 50 mM NaCl, and 50 μM L-Leu.